

# Asymmetric coherent transmission for single particle diode and gyroscope

S. Yang,<sup>1</sup> Z. Song,<sup>2</sup> and C. P. Sun<sup>1</sup>

<sup>1</sup>Key Laboratory of Frontiers in Theoretical Physics, Institute of Theoretical Physics,  
Chinese Academy of Sciences, Beijing 100190, China

<sup>2</sup>School of Physics, Nankai University, Tianjin 300071, China

We study the single particle scattering process in a coherent multi-site system consisting of a tight-binding ring threaded by an Aharonov-Bohm flux and several attaching leads. The asymmetric behavior of scattering matrix is discovered analytically in the framework of both Bethe Ansatz and Green's function formalism. It is found that, under certain conditions, a three-site electronic system can behave analogous to a perfect semiconductor diode where current flows only in one direction. The general result is also valid for a neutral particle system since the effective magnetic flux may be implemented by a globe rotation. This observation means that the three-site system can serve as an orientation measuring gyroscope due to the approximate linear dependence of the current difference of two output leads on the rotational angular velocity.

PACS numbers: 73.23.-b, 05.60.Gg, 85.35.Ds

## I. INTRODUCTION

Single particle quantum devices work essentially in a quantum mechanical way by using the whole features of quantum states, especially the phases of quantum states. A typical example is the single electron transistor (SET) [1, 2, 3, 4, 5] and its photon analogue [6, 7], which plays a central role in quantum manipulation and quantum measurement. A SET is a mesoscopic system that allows confined electrons to tunnel to the metallic leads. It turns on and off again every time one electron is added to the isolated region [2]. Unlike the conventional transistors, which can be understood by using classical concepts, the SET is a quantum mechanical one in substance. It can be utilized for measuring the quantum effects in Josephson junction superconductor circuit and nano-mechanics resonators [8, 9, 10].

In this article, we will pay attention to another single particle quantum device, which can be understood as the quantum analogue of the conventional diode device. In practice, diode devices are indispensable for building various electronic circuits in the traditional electronics. Accordingly, once a coherent diode device has been implemented, a single-particle quantum circuit may be further realized in the level of single quantum state by using of the two basic elements, single particle transistor and diode. Compared with the traditional electrocircuits based on the density distribution of electrons, the new quantum circuit makes full use of the quantum properties including quantum phases in information processing. In this sense, we can also regard it as a necessary element in quantum information science and technology.

A major research effort in recent years is to seek a simplest single particle system with diode features [11, 12, 13, 14], which is characterized by the asymmetric performance of transmission coefficients along the opposite directions. In the present investigation, we find that a three-site tight-binding ring system threaded by an Aharonov-Bohm (AB) magnetic flux has analogy to a perfect diode in a wide range of parameters.

In addition, our studies are not restricted to the charged particle case. For a neutral particle system, an effective magnetic

flux is induced by applying a globe rotation [15], which can also break the time reversal symmetry and lead to the asymmetric transmissions. It is shown that the difference of the two output currents is linearly proportional to the rotational angular velocity approximately, which behaves as a new kind of extended Sagnac gyroscope [16, 17].

Decades ago, Büttiker *et al.* have found that the conductance of a multi-terminal sample is asymmetric in the presence of an AB flux [18, 19, 20]. Realization of such mechanism in quantum device requires its size being smaller than the phase-breaking length. Thus seeking a minimized system with asymmetric feature is attractive in practice. A discrete system may be a good candidate to accomplish such a task. It is of both theoretical and practical importance to study this theory in a discrete system. Moreover, we show practical applications of the quantum interference effect as single electron diode and single particle gyroscope. In the general discussion part, it is interesting to find that some special configurations may protect the transmission coefficients from symmetry breaking even if the AB magnetic flux is imposed.

This paper is organized as follows. In Sec. II, the general  $N$ -site ring-shaped model with attaching leads is presented, and an analytical method for calculating the transmission coefficients is introduced. In Sec. III, we study the asymmetric transmission behavior of the 3-site system by using the exact solution. In Sec. IV, a single particle gyroscope and its physical realization in optical lattice is proposed. In Sec. V, we give a general discussion about the condition of asymmetric transmission by making use of Green's function approach, which also confirms the results obtained above. Conclusions are summarized at the end of the paper. In the appendix, a proof is given to show the equivalence between the Bethe Ansatz and the Green's function method.

## II. MODEL AND ITS EXACT SOLUTION

The central system we concern is described by an  $N$ -site tight-binding ring threaded by a magnetic flux shown in Fig.

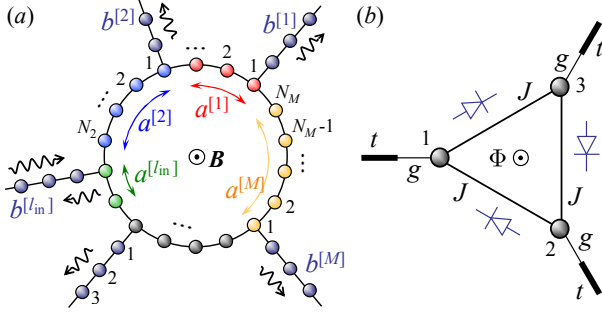


FIG. 1: (color online) (a) Configuration of the ring shaped scattering system including  $M$  arc chains  $\{a^{[1]}, a^{[2]}, \dots, a^{[M]}\}$  and  $M$  attaching leads  $\{b^{[1]}, b^{[2]}, \dots, b^{[M]}\}$  threaded by a magnetic flux. The input and possible output currents are marked by wavy arrows. (b) Schematic illustration of the three-site chiral coherent scattering system with diode features.

1(a). The Hamiltonian reads

$$H_C = -J \sum_{j=1}^N (e^{i\phi_j} a_j^\dagger a_{j+1} + \text{H.c.}) + \omega \sum_{j=1}^N a_j^\dagger a_j. \quad (1)$$

Here,  $a_j^\dagger$  ( $a_j$ ) is the fermion creation (annihilation) operator at the  $j$ th site. The external magnetic field does not exert force on the Bloch electrons, but makes hopping integral  $J$  between sites  $j$  and  $(j+1)$  pick up an AB phase factor  $\exp(i\phi_j)$  in the Peierls approximation [21], where

$$\phi_j = \frac{2\pi}{\phi_0} \int_j^{j+1} \mathbf{A} \cdot d\mathbf{l}, \quad (2)$$

$\phi_0 = hc/e$  is the flux quanta and  $\Phi = \sum_{j=1}^N \phi_j$  is the total magnetic flux;  $\omega$  is the chemical potential of the central system. In the same figure,  $M$  half-infinite tight-binding leads are attached to  $M$  sites on the ring, and the corresponding Hamiltonian are

$$H_L = \sum_{l=1}^M H_l = - \sum_{l=1}^M \left( g a_{j_l}^\dagger b_1^{[l]} + t \sum_i b_i^{\dagger[l]} b_{i+1}^{[l]} + \text{H.c.} \right). \quad (3)$$

Without loss of generality, we let  $l = l_{in}$  lead as the input lead, while all the other indexed  $l \neq l_{in}$  leads are output ones. The spin degree of freedom is omitted for notational brevity here since the model does not contain interaction involving spin.

In order to investigate the scattering problem through such a system in the framework of Bethe Ansatz [7, 22, 23] more efficiently, we regard the  $N$ -site ring as  $M$  arc tight-binding chains connected by the head and tail. As illustrated in Fig. 1(a), the length of the  $l$ th arc chain  $a^{[l]}$  is  $N_l$ , and the  $l$ th lead  $b^{[l]}$  is joined with the 1th site of the  $l$ th arc chain. The total number of sites on the ring satisfies  $\sum_{l=1}^M N_l = N$ . Then the Hamiltonian  $H = H_C + H_L$  is rearranged with

$$H_C = -J \sum_{l=1}^M \left[ \sum_{j=1}^{N_l-1} e^{i\phi_j^{[l]}} a_j^\dagger a_{j+1}^{[l]} + e^{i\phi_{N_l-1}^{[l]}} a_{N_l-1}^\dagger a_1^{[l]} + \text{H.c.} \right],$$

$$H_L = - \sum_{l=1}^M \left( g a_1^{\dagger[l]} b_1^{[l]} + t \sum_i b_i^{\dagger[l]} b_{i+1}^{[l]} + \text{H.c.} \right). \quad (4)$$

The scattering wave function is supposed to be

$$\begin{aligned} \psi_a^{[l]}(j) &= A_1(l) e^{i(qj - \sum_{m=1}^{j-1} \phi_m^{[l]})} + A_2(l) e^{-i(qj + \sum_{m=1}^{j-1} \phi_m^{[l]})}, \\ \psi_b^{[l]}(j) &= B(l) e^{ikj} + \delta_{l, l_{in}} e^{-ikj}, \end{aligned} \quad (5)$$

where  $B(l_{in})$  actually defines the reflection coefficient

$$R_{l_{in}} = |B(l_{in})|^2, \quad (6)$$

while  $B(l)$  for  $l \neq l_{in}$  give the transmission coefficient from the  $l_{in}$ th lead to the  $l$ th lead,

$$T_{l_{in}, l} = |B(l)|^2 \quad (7)$$

The coefficients  $A_1(l)$ ,  $A_2(l)$  and  $B(l)$  should satisfy the connecting conditions and the Schrödinger equation

$$\begin{aligned} \psi_a^{[l-1]}(N_{l-1} + 1) &= \psi_a^{[l]}(1), \\ -g\psi_b^{[l]}(1) - J \left[ e^{i\phi_1^{[l]}} \psi_a^{[l]}(2) + e^{-i\phi_{N_{l-1}}^{[l-1]}} \psi_a^{[l-1]}(N_{l-1}) \right] \\ &= (E - \omega) \psi_a^{[l]}(1), \\ -t\psi_b^{[l]}(2) - g\psi_a^{[l]}(1) &= E\psi_b^{[l]}(1). \end{aligned} \quad (8)$$

The relation between  $k$  and  $q$  is also given by the Schrödinger equation,

$$\begin{aligned} -J \left[ e^{i\phi_j^{[l]}} \psi_a^{[l]}(j+1) + e^{-i\phi_{j-1}^{[l]}} \psi_a^{[l]}(j-1) \right] &= (E - \omega) \psi_a^{[l]}(j), \\ -t \left[ \psi_b^{[l]}(j+1) + \psi_b^{[l]}(j-1) \right] &= E\psi_b^{[l]}(j), \end{aligned} \quad (9)$$

for  $j \neq 1$ , i.e.,

$$E = -2t \cos k = -2J \cos q + \omega. \quad (10)$$

Then the  $3M$  coefficients  $\{A_1(l), A_2(l), B(l)\}$  are fully determined by solving the above  $3M$  independent equations in Eq. (8). It shows that the Bethe Ansatz method can provide the exact wave function of the scattering state. For small size system, the explicit wave function allows us to clarify the mechanism of the asymmetric transmission from the viewpoint of interference.

### III. ASYMMETRIC COHERENT TRANSMISSION

Hereafter, we mainly consider the simplest case of  $N = 3$  and  $M = 3$  shown in Fig. 1(b). The Bethe Ansatz approach gives the exact solution of transmission and reflection coefficients as

$$\begin{aligned} T_{13} &= T_{32} = T_{21} = T_R, \\ T_{12} &= T_{23} = T_{31} = T_L, \\ R_1 &= R_2 = R_3 = 1 - T_{12} - T_{13} = R, \end{aligned} \quad (11)$$

where

$$\begin{aligned} T_R &= \frac{4g^4 J^2 t^2}{\Xi} \sin^2 k |Jte^{-i\Phi} + \Theta|^2, \\ T_L &= \frac{4g^4 J^2 t^2}{\Xi} \sin^2 k |Jte^{i\Phi} + \Theta|^2, \\ \Theta &= 2t^2 \cos k - g^2 e^{ik} + t\omega, \\ \Xi &= |2J^3 t^3 \cos \Phi + 3J^2 t^2 \Theta - \Theta^3|^2. \end{aligned} \quad (12)$$

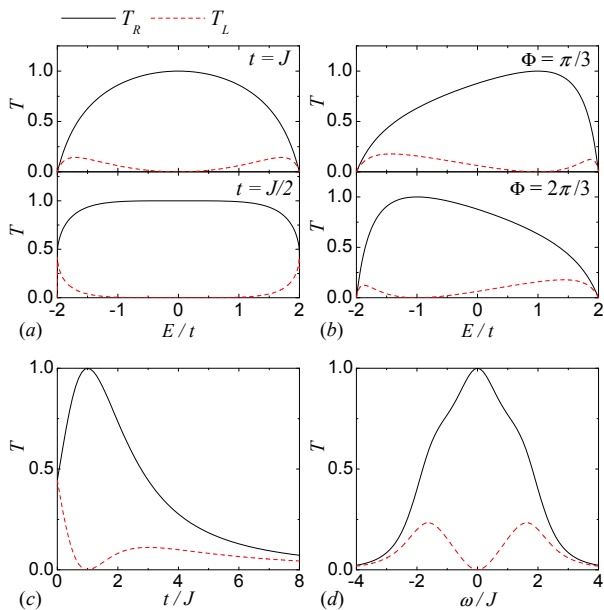


FIG. 2: (color online) Typical cases of transmission coefficients in the clockwise direction  $T_R$  (black solid lines) and anti-clockwise direction  $T_L$  (red dashed lines). (a)  $T_R$  and  $T_L$  with respect to  $E/t$  in the case of  $t = J$  (upper panel) and  $t = J/2$  (lower panel), where  $g^2/t = J$ ,  $\Phi = \pi/2$ , and  $\omega = 0$ . It shows that the system behaves like a perfect diode at  $E = 0$  (upper panel) and within a wide range  $E \in [-t, t]$  (lower panel). (b) Transmission spectrum in the case of  $g = t = J$  and  $\omega = 0$  with  $\Phi = \pi/3$  (upper panel) and  $\Phi = 2\pi/3$  (lower panel). The perfect diode energy can be adjusted by the magnetic flux  $\Phi$ . (c) Plots of  $T_R$  and  $T_L$  at  $E = 0$  as a function of  $t/J$  with parameters  $g = t$ ,  $\Phi = \pi/2$  and  $\omega = 0$ . The transmission coefficients of two directions coincide in the limit of both  $t \rightarrow 0$  and  $t \rightarrow \infty$ , but diverge dramatically at the critical point  $t = J$ . (d) When  $g^2/t = J$ ,  $\Phi = \pi/2$ , and  $E = 0$ , the diode feature is optimal at the resonant point  $\omega/J = 0$ .

We notice that in general, the transmission coefficients  $T_R$  and  $T_L$  from one lead to the other two are not identical, i.e., the current flow across two arbitrary leads is unidirectional. On the other hand, the clockwise coefficients  $T_{13}, T_{32},$  and  $T_{21}$ , defined as  $T_R$ , have the same value, so do the anti-clockwise coefficients  $T_{12}, T_{23}, T_{31}$  defined as  $T_L$ . Namely, the transmission coefficients have dextrorotary and levorotary characteristics. We will discuss the general asymmetric scattering problem in detail in Sec. V. We will see that this kind of feature is reasonable for a non-bipartite system with broken time-reversal symmetry induced by the external magnetic flux.

Now we concentrate on some special cases of the 3-site ring to exemplify this feature.

(1)  $g^2/t = J$ ,  $\Phi = \pi/2$ , and  $\omega = 0$ , the Bloch electrons are injected at  $E = 0$  with momentum  $k = \pi/2$ . Eq. (11) and (12) becomes

$$T_R = 1, T_L = 0, R = 0. \quad (13)$$

It means that the current can only flow in the clockwise direction with no reflection. Thus the system is a perfect diode if we regard the 1th lead as the source and 2th lead as the drain.

The profiles of the corresponding transmission spectra,  $T_R$  and  $T_L$  as functions of  $E$  for  $t = J$  and  $t = J/2$ , are plotted in Fig. 2(a). One can see that, when  $t = J/2$  and  $g^2/t = J$ , the diode is perfect even if the input energy  $E$  is shifted within the region  $[-t, t]$ . This shows the great tolerant as a perfect quantum device.

(2)  $g = t = J$  and  $\omega = 0$ , the input energy is determined by  $k$  as  $E = -2t \cos k$ ,

$$\begin{aligned} T_R &= 1, T_L = 0, R = 0, \text{ for } k = \pi - \Phi + 2n\pi, \\ T_R &= 0, T_L = 1, R = 0, \text{ for } k = \Phi - \pi + 2n\pi, \\ T_R &= 0, T_L = 0, R = 1, \text{ for } k = n\pi. \end{aligned} \quad (14)$$

Therefore, for a given  $E$ , we can get a perfect diode device by tuning  $\Phi$ . The transmission spectrum of the  $\Phi = \pi/3$  and  $2\pi/3$  cases are shown in 2(b) to give a visual impression.

(3)  $g = t$ ,  $\Phi = \pi/2$  and  $\omega = 0$ , we plot  $T_R$  and  $T_L$  at  $E = 0$  with respect to  $t$  in Fig. 2(c). The point of  $t = J$  denotes the diode case. Beyond that critical point, the difference between  $T_R$  and  $T_L$  gets smaller. In the limit of  $t \rightarrow 0$ ,  $T_R$  and  $T_L$  converged to  $4/9$ .

(4)  $g^2/t = J$ ,  $\Phi = \pi/2$ , and  $E = 0$ . The dependence of  $T_R$  and  $T_L$  on the frequency detuning  $\omega$  is shown in Fig. 2(d). It is apparent that the resonant case is advantageous to forming a perfect diode.

A diode system based on the above mechanism is different from the classical ones in semiconductor electronics. The conventional diode such as P-N junction is made up based on the different density distribution of electrons in the p-type and n-type materials. When the external voltage is absent and the equilibrium is reached, there is a difference of chemical potentials between the two materials. Consequently, current will flow readily in the forward biased direction since the applied voltage decreases the barrier; but not in the reverse biased direction because the barrier is raised. By contrast, the single particle diode device presented here works in the region with no chemical potential difference. It makes full use of the pure quantum interference phenomenon induced by the Aharonov-Bohm effect.

#### IV. SINGLE PARTICLE GYROSCOPE

So far we have seen that the threaded magnetic flux plays an important role in controlling the amount and direction of currents. It can be applicable to the more extended system. Actually, if the system is rotated, an effective magnetic field will be induced in the rotating frame of references. Therefore, the difference between the currents of the two output leads can reflect the rotational angular velocity of the system. That is the basic idea of making up a gyroscope by using the above mentioned asymmetric scattering system. The analysis below can be applied to a neutral-particle system by simply choosing  $\phi = 0$ .

For a rotating system with angular frequency  $\Omega$ , an additional term

$$H_R = -\Omega L_z = -\Omega K \sum_{j=1}^N \left( i e^{i\phi_j} a_j^\dagger a_{j+1} + \text{H.c.} \right), \quad (15)$$

should be added on the Hamiltonian [15] in the non-inertial frame, where  $K$  is a constant depends on the geometry of the central system. In the meantime, the Hamiltonian of leads  $H_L$  remains the same since the leads are along the radial directions. Then the Hamiltonian of the central system becomes  $H'_C = H_C + H_R$  or

$$H'_C = -J_\Omega \sum_{j=1}^N \left[ e^{i(\phi_j + \phi_\Omega)} a_j^\dagger a_{j+1} + \text{H.c.} \right], \quad (16)$$

where  $J_\Omega = \sqrt{J^2 + \Omega^2 K^2}$ ,  $\tan \phi_\Omega = \Omega K / J$ . The total effective magnetic flux

$$\Phi_\Omega = \sum_{j=1}^3 \phi_j + 3\phi_\Omega = \Phi + 3\phi_\Omega \quad (17)$$

depends on the angular frequency  $\Omega$ . For simplicity, we only focus on the case of  $E = 0$  injection. If the total effective magnetic flux is absent, i.e.,  $\Phi_\Omega = 0$ , the transmission and reflection are symmetric due to the fact  $T_R = T_L = T(\omega)$  with

$$T(\omega) = \frac{4g^4 J^2 t^2}{\left[ g^4 + t^2 (\omega - 2J)^2 \right] \left[ g^4 + t^4 (\omega + J)^2 \right]}. \quad (18)$$

Then we have  $\Delta = T_R - T_L = 0$ , which characterizes the asymmetrical feature. For small effective magnetic flux  $\Phi_\Omega \approx 0$ , we have

$$\Delta = \frac{4Jtg^2 T(\omega)}{g^4 + t^4 (\omega + J)^2} \Phi_\Omega + O(\Phi_\Omega)^3, \quad (19)$$

i.e., the current difference  $\Delta$  is a linear function of  $\Phi_\Omega$  in the vicinity of  $\Phi_\Omega = 0$ . For a typical case  $g = \sqrt{Jt}$ , we plot  $\Delta$  as a function of  $\Phi_\Omega$  in Fig. 3(a). In the resonant case  $\omega = 0$ , it shows that this gyroscope have the advantage of good linear response within a wide range of  $\Phi_\Omega$ . In practice, in the case of extremely large rotation frequency  $\Omega$ , a compensate magnetic flux can be added to ensure it works in the linear region. For some off-resonant cases, e.g.,  $\omega = -0.8J$ , the ratio of  $\Delta$  to  $\Phi_\Omega$  at  $\Phi_\Omega = 0$  is larger than the one of the resonant case. The larger ratio implies a higher sensitivity, so it is good for measurement.

As a result, the instantaneous value  $\Omega(t)$  can be obtained by measuring  $\Delta(t)$  directly. The cumulative rotation angle is just an integration of the angular velocity over time,

$$\theta(\tau) = 2\pi \int_0^\tau \Omega(t) dt. \quad (20)$$

Therefore, such a system can measure the angular velocity and orientation precisely as a gyroscope.

Actually, the most famous modern gyroscope is the laser gyroscope based on Sagnac effect [16, 17] (Two waves propagating along the opposite directions though a closed rotating

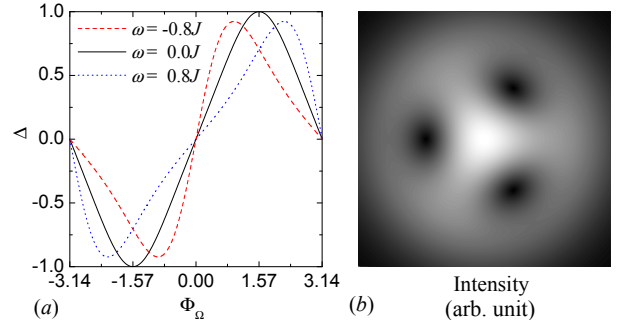


FIG. 3: (color online) (a) The difference of the transmission coefficients on two directions  $\Delta$  depends linearly on the total effective magnetic flux  $\Phi_\Omega$  around  $\Phi_\Omega = 0$  approximately. Here,  $g^2/t = J$ ,  $E = 0$ , the frequency detuning  $\omega$  is chosen as  $\omega = -0.8J$  (red dashed line),  $\omega = 0$  (black solid line), and  $\omega = 0.8J$  (blue dot line). (b) Intensity distribution of the three-site ring-shaped optical lattice generated by two Laguerre-Gauss laser beams.

ring will induce a relative phase difference, and the position of the interference fringes depends on the angular velocity). Our proposal is an extension of the Sagnac gyroscope since the interference effect is also used. However, the difference of the two output currents is measured here instead of observing the interference pattern directly, which may enhance the sensitivity of the results.

Our asymmetric coherent scattering system may be realized by trapping atoms in a ring-shaped optical lattice. The optical lattices with periodic boundary condition have been produced by the superposition of two Laguerre-Gauss (LG) laser modes theoretically and experimentally [25, 26]. The LG beam with frequency  $\omega$ , wave vector  $k$ , and amplitude  $E_0$  propagating along the  $z$  axis has the form

$$LG_l^p(\omega) = E_0 f_{pl}(r) e^{i\theta l} e^{i(\omega t - kz)},$$

$$f_{pl}(r) = (-1)^p \sqrt{\frac{2p!}{\pi(p+|l|)!}} x^{|l|} L_p^l(x^2) e^{-x^2/2}, \quad (21)$$

where  $x = \sqrt{2}r/r_0$  and  $r_0$  is the beam waist.  $L_p^l(\cdot)$  is the generalized Laguerre polynomial. To generate a 1D optical lattice ring with  $N$  traps, parameters are chosen as  $p_1 = p_2 = 0$ ,  $l_1 = 0$ ,  $l_2 = N$ , and  $x_1 = 1.3x_2$ . The intensity distribution of the  $N = 3$  case is shown in Fig. 3(b).

## V. GREEN'S FUNCTION APPROACH AND GENERAL DISCUSSION FOR ASYMMETRIC TRANSMISSION

In this section, we generally consider in which case the asymmetric transmission can happen for a general multi-terminal tight-binding system. For an arbitrary single-particle tight-binding model with attaching leads, we will derive the condition of the asymmetric transmission  $T_{pq} \neq T_{qp}$  between lead  $p$  and  $q$  by using the Green's function formalism introduced in Ref. [24] and references therein.

We first briefly review Green's function method for multi-terminal system. The retarded Green's function of the system

as a function of input energy  $E = -2t \cos k$  is

$$G^R = \frac{1}{E - H_C - \Sigma_{leads}}, \quad (22)$$

where  $H_C$  is the Hamiltonian of the central system, and  $\Sigma_{leads}$  as the total self-energy denotes the contribution of the half-infinite leads,  $\Sigma_{leads} = \sum_{p \in \{\text{lead}\}} \Sigma_p$ . On the single particle basis  $\{a_1^\dagger |0\rangle, a_2^\dagger |0\rangle, \dots, a_N^\dagger |0\rangle\}$ , both  $H_C$  and  $\Sigma_p$  are  $N \times N$  matrix. Especially, each  $\Sigma_p$  has only one non-zero matrix element at the cross point of row  $p$  and column  $p$ ,

$$(\Sigma_p)_{p,p} = -\frac{g^2}{t} e^{ik(E)} = \Sigma_0, \quad (23)$$

which is because the  $p$ th lead is only attached to the  $p$ th site of the central system via  $(-ga_p^\dagger b_1^{[p]} + \text{H.c.})$ . Then the advanced Green's function  $G^A = G^{R\dagger}$  and  $\Gamma_p$  matrix  $\Gamma_p = i[\Sigma_p - \Sigma_p^\dagger]$  are obtained sequentially. The transmission spectrum from lead  $p$  to lead  $q$  ( $q \neq p$ ) is given by

$$T_{pq} = \text{Tr} [\Gamma_q G^R \Gamma_p G^A]. \quad (24)$$

Applying it to the ring system mentioned in Sec. II-IV, one can see that the Green's function formalism gives the same exact solution as the one form Bethe Ansatz method. The equivalence of the two approaches is proved in the appendix.

In general, the Green's functions  $G^R$  (Eq. (22)) and  $G^{R\dagger}$  are complex. From Eq. (24), the transmission coefficient  $T_{pq}$  is

$$\begin{aligned} T_{pq} &= \text{Tr} [\Gamma_q (\text{Re} G^R + i \text{Im} G^R) \Gamma_p (\text{Re} G^{R\dagger} + i \text{Im} G^{R\dagger})] \\ &= (\Gamma_q)_{qq} \text{Re}(G^R)_{qp} (\Gamma_p)_{pp} \text{Re}(G^{R\dagger})_{pq} \\ &\quad - (\Gamma_q)_{qq} \text{Im}(G^R)_{qp} (\Gamma_p)_{pp} \text{Im}(G^{R\dagger})_{pq} \\ &= (\Gamma_p)_{pp} (\Gamma_q)_{qq} [\text{Re}(G^R)_{qp}^2 + \text{Im}(G^R)_{qp}^2] \\ &= (\Gamma_p)_{pp} (\Gamma_q)_{qq} |(G^R)_{qp}|^2, \end{aligned} \quad (25)$$

where we have use the identity

$$\begin{aligned} \text{Re}(G^R)_{qp} &= \text{Re}(G^{R\dagger})_{pq}, \\ \text{Im}(G^R)_{qp} &= -\text{Im}(G^{R\dagger})_{pq}, \end{aligned} \quad (26)$$

together with the property that the  $\Gamma$  matrix has only one non-zero matrix element. Similarly, for the inverse transport,

$$T_{qp} = (\Gamma_p)_{pp} (\Gamma_q)_{qq} |(G^R)_{pq}|^2. \quad (27)$$

Therefore, once

$$|(G^R)_{qp}| = |(G^R)_{pq}|, \quad (28)$$

we have a symmetric scattering  $T_{pq} = T_{qp}$ . When this condition is not satisfied, i.e.,  $|(G^R)_{qp}| \neq |(G^R)_{pq}|$ , an asymmetric scattering is obtained. Eq. (22) tells us that the condition is not only related to the intrinsic symmetry of the central Hamiltonian  $H$ , but also depends on the features of the leads. For example, if we only attach two leads on the same 3-site central ring investigated in Sec. III, the asymmetric transmission

phenomena will disappear. This result is in agreement with the viewpoint in Ref. [20] that the simplest example must involve at least three channels.

Since  $H_C$  is Hermitian and  $\Sigma_{leads}$  is diagonal, the term

$$H_{eff} = E - H_C - \Sigma_{leads} \quad (29)$$

can be written as a matrix as

$$H_{eff} = \begin{pmatrix} c_1 & d_{12} & d_{13} & \cdots & d_{1N} \\ d_{12}^* & c_2 & d_{23} & \cdots & d_{2N} \\ d_{13}^* & d_{23}^* & \ddots & & \vdots \\ \vdots & \vdots & & c_{N-1} & d_{N-1,N} \\ d_{1N}^* & d_{2N}^* & \cdots & d_{N-1,N}^* & c_N \end{pmatrix}. \quad (30)$$

The diagonal matrix elements are noted by  $c$ , while the off-diagonal ones are denoted by  $d$ . The inverse matrix of  $H_{eff}$  has the form

$$G^R = \frac{D}{\text{Det}(H_{eff})}, \quad (31)$$

where  $D = \text{Adj}(H_{eff})$  is the adjugate matrix of  $H_{eff}$ , which is the transpose of the matrix of cofactors. Since the determinant  $\text{Det}(H_{eff})$  is a constant, our problem is reduced to the condition of the identity  $|D_{qp}| = |D_{pq}|$ . Since a matrix and its transpose have the same determinant, we notice that  $D_{qp}$  and  $D_{pq}$  have the form

$$\begin{aligned} D_{qp} &= F(c_1, \dots, c_N; d_{12}, \dots, d_{N-1,N}; d_{12}^*, \dots, d_{N-1,N}^*), \\ D_{pq} &= F(c_1, \dots, c_N; d_{12}^*, \dots, d_{N-1,N}^*; d_{12}, \dots, d_{N-1,N}). \end{aligned} \quad (32)$$

Here,  $F$  is a polynomial function constructed by  $c$  and  $d$ . Generally speaking, if all of the  $c$  and  $d$  are non-zero random complex numbers,  $|D_{qp}|$  is probably not equal to  $|D_{pq}|$ . However, under some specific conditions, the asymmetric transmission will disappear. Now we focus on the resonant systems (there is no chemical potential difference between the leads and the central lattice) and take some typical cases as an illustration.

(1) Obviously, when there is no external magnetic flux breaks the time reversal symmetry, we have all the  $d = d^*$ , then  $D_{qp} = D_{pq}$ , the condition Eq. (28) is automatically satisfied.

(2) When all the  $c$  are real, i.e.,  $c = c^*$ ,  $D_{qp} = D_{pq}^*$ , the condition Eq. (28) is also satisfied. Because of Eq. (23) and (10), this case requires that the incident momentum  $k$  is either 0 or  $\pi$ , which corresponds to injecting an electron at the top or bottom of the Bloch energy band. Thus it is not very easy to be realized in practice.

(3) A realizable but not trivial case: The symmetric scattering can be obtained even though the magnetic field is present if the geometry of the lattice is bipartite and electrons are injected at  $E = 0$ . A bipartite lattice is a lattice that can be divided into A and B sublattices, such that a site in A is connected only with sites in B and vice versa. At this time, the function  $F$  is a polynomial contains only either even order of  $c$  or odd order of  $c$ . In other words, if one term of  $F$  is a product of even number of  $c$  and some  $d$ , no term of  $F$  contains the

product of odd number of  $c$ , thus  $F$  is called even with respect to  $c$ . The situation is similar when  $F$  is odd with respect to  $c$ . The momentum for  $E = 0$  is  $k = \pi/2$ , then all the  $c$  are pure imaginary,  $c = -c^*$ . Therefore,  $D_{qp} = (-1)^{\text{even}} D_{pq}^*$  if  $F$  is even with respect to  $c$ , while  $D_{qp} = (-1)^{\text{odd}} D_{pq}^*$  if  $F$  is odd with respect to  $c$ . For both cases, we have  $|(G^R)_{qp}| = |(G^R)_{pq}|$  which represents a symmetric scattering.

(4) For the bipartite central lattice,  $T_{qp}$  equals to  $T_{pq}$  even though the input energy  $E \neq 0$  if one of the following conditions is satisfied. (i)  $N$  is odd, there is no lead connected to the sublattice with  $(N - 1)/2$  sites, or there are no more than two leads connected to the sublattice with  $(N + 1)/2$  sites. (ii)  $N$  is even, there are no more than one lead connected to either sublattice A or sublattice B.

## VI. CONCLUSION

In this paper, we take the three-site tight-binding ring as an explicit example to study the scattering problem of some coherent nanostructure with or without time reversal symmetry by virtue of exact solutions. It is discovered that, induced by the threaded or effective magnetic flux, the asymmetric transmission can happen in such a system. With this interesting property, on the one hand, such a system behaves as a quantum diode for a charged particle due to the pure quantum interference effect. On the other hand, it can also be served as a gyroscope for either a charged or neutral particle when a global rotation providing an effective magnetic flux. We have shown that the difference of the output currents is linear proportional to the rotational angular velocity approximately. The observable effects presented in this paper are hopeful to be realized experimentally in the quantum dot system and the ultra-cold atom optical lattice system. We also try to generalize the results from the three-site system to the general ones. According to the Green's function approach [24], it is demonstrated that the intrinsic symmetries of the whole system, including the geometry of lattice and leads, determine the symmetry of scattering coefficients together. Protected by the bipartite configuration, a symmetry scattering may be obtained even if the time reversal symmetry is broken for the central system.

### Acknowledgments

This work is supported by NSFC No. 10474104, 60433050, 10874091 and No. 10704023, NFRPC No. 2006CB921205 and 2005CB724508.

### APPENDIX: EQUIVALENCE BETWEEN BETHE ANSATZ METHOD AND GREEN'S FUNCTION METHOD

In this appendix, we prove that the Bethe Ansatz method and Green's function method are equivalent for determining the transmission coefficients.

The Hamiltonian of a general central system with  $N$  sites reads

$$H_C = \sum_{j,j'=1}^N (H_C)_{j,j'} a_j^\dagger a_{j'}. \quad (\text{A.1})$$

We suppose that there is a set of  $j$  defined as  $\{\text{lead}\} = \{j_1, j_2, \dots, j_M\}$ , where  $2 \leq M \leq N$ . If  $j \in \{\text{lead}\}$ , a half infinite tight-binding lead is attached to the  $j$ th site. The total Hamiltonian of leads is

$$H_L = - \sum_{j \in \{\text{lead}\}} \left( g a_j^\dagger b_1^{[j]} + t \sum_{j'=1}^{\infty} b_{j'}^{[j]} b_{j'+1}^{[j]} + \text{H.c.} \right). \quad (\text{A.2})$$

According to the Bethe Ansatz method, the scattering state is supposed to be

$$|\psi\rangle = \sum_j \psi_a(j) a_j^\dagger |0\rangle + \sum_{j \in \{\text{lead}\}} \sum_{j'} \psi_b^{[j]}(j') b_{j'}^{[j]} |0\rangle, \quad (\text{A.3})$$

where

$$\psi_b^{[j]}(j') = B(j) e^{ikj'} + \delta_{j,p} e^{-ikj'}. \quad (\text{A.4})$$

The  $p$ th lead has been chosen as the input lead. From the Schrödinger equation

$$(H_C + H_L) |\psi\rangle = E |\psi\rangle, \quad (\text{A.5})$$

$\psi_a(j)$  and  $\psi_b^{[j]}(j)$  should satisfy

$$\sum_{j'} (H_C)_{j,j'} \psi_a(j') - g \delta_{j, \{\text{lead}\}} \psi_b^{[j]}(1) = E \psi_a(j) \quad (\text{A.6})$$

for any  $j$ , and

$$\begin{aligned} -g \psi_a(j) - t \psi_b^{[j]}(2) &= E \psi_b^{[j]}(1), \\ -t [\psi_b^{[j]}(j' + 1) + \psi_b^{[j]}(j' - 1)] &= E \psi_b^{[j]}(j') \end{aligned} \quad (\text{A.7})$$

for  $j \in \{\text{lead}\}$ . Eq. (A.4) and (A.7) give the dispersion relation

$$E = -2t \cos k, \quad (\text{A.8})$$

together with the equation for  $j \in \{\text{lead}\}$ ,

$$\frac{g}{t} \psi_a(j) = B(j) + \delta_{j,p}. \quad (\text{A.9})$$

For future convenience, we define a column vector  $X$ ,

$$\begin{aligned} X &= (X_1 \ X_2 \ \dots \ X_N)^T, \\ X_j &= (1 - \delta_{j, \{\text{lead}\}}) \left( \frac{g}{t} \psi_a(j) \right) + \delta_{j, \{\text{lead}\}} B(j). \end{aligned} \quad (\text{A.10})$$

Eq. (A.6) can be simplified as

$$\begin{aligned} &\sum_{j'} \left[ E \delta_{j,j'} - (H_C)_{j,j'} - \left( -\frac{g^2}{t} e^{ik} \delta_{j,j'} \delta_{j, \{\text{lead}\}} \right) \right] X_{j'} \\ &= (H_C)_{j,p} - \delta_{j,p} \left( E + \frac{g^2}{t} e^{-ik} \right), \end{aligned} \quad (\text{A.11})$$

which is a system of linear equations in the variables  $X_j$ . In the matrix form, Eq. (A.11) becomes

$$H_{eff}X = W, \quad (\text{A.12})$$

where

$$H_{eff} = E - H - \Sigma_{leads}. \quad (\text{A.13})$$

The matrix elements of  $H_{eff}$ ,  $W$ , and  $\Sigma_{leads}$  are

$$\begin{aligned} (H_{eff})_{j,j'} &= E\delta_{j,j'} - (HC)_{j,j'} - \left(-\frac{g^2}{t}e^{ik}\delta_{j,j'}\delta_{j,\{lead\}}\right), \\ W_j &= (HC)_{j,p} - \delta_{j,p}\left(E + \frac{g^2}{t}e^{-ik}\right), \\ (\Sigma_{leads})_{j,j'} &= -\frac{g^2}{t}e^{ik}\delta_{j,j'}\delta_{j,\{lead\}} = \Sigma_0\delta_{j,j'}\delta_{j,\{lead\}}, \end{aligned} \quad (\text{A.14})$$

where  $\Sigma_0 = -(g^2/t)e^{ik}$ . The solution of  $X_j$  can be given by the Cramer's rule [27]. Without loss of generality, we focus on the solution of  $X_q$  with  $q \in \{\text{lead}\}$  but  $q \neq p$ ,

$$X_q = B(q) = \frac{\text{Det}(H_{eff}^{(q)})}{\text{Det}(H_{eff})}. \quad (\text{A.15})$$

Here, the matrix elements of  $H_{eff}^{(q)}$  are

$$(H_{eff}^{(q)})_{j,j'} = (1 - \delta_{j',q})(H_{eff})_{j,j'} + \delta_{j',q}W_j. \quad (\text{A.16})$$

The determinant of  $H_{eff}^{(q)}$  equals to the one of another matrix  $H_{eff}^{(q)'}$ , where

$$\begin{aligned} (H_{eff}^{(q)'})_{j,j'} &= (1 - \delta_{j',q})(H_{eff})_{j,j'} + \delta_{j',q}W_j + \delta_{j',q}(H_{eff})_{j,p} \\ &= (1 - \delta_{j',q})(H_{eff})_{j,j'} + i\delta_{j,p}\delta_{j',q}\Gamma_0, \end{aligned} \quad (\text{A.17})$$

and

$$\Gamma_0 = i(\Sigma_0 - \Sigma_0^*) \quad (\text{A.18})$$

is a real number. So that

$$\text{Det}(H_{eff}^{(q)}) = \text{Det}(H_{eff}^{(q)'}) = i\Gamma_0\Lambda_{pq}. \quad (\text{A.19})$$

$\Lambda_{pq}$  is the  $(p, q)$ th algebraic cofactor of  $H_{eff}$ , which is actually  $(-1)^{p+q}$  times the determinant of the submatrix obtained by removing  $p$ th row and  $q$ th column from  $H_{eff}$ . Therefore, the transmission coefficient from lead  $p$  to lead  $q$  is

$$T_{pq} = |B(q)|^2 = \left|\frac{i\Gamma_0\Lambda_{pq}}{\text{Det}(H_{eff})}\right|^2 = \Gamma_0^2 \left|\frac{\Lambda_{pq}}{\text{Det}(H_{eff})}\right|^2. \quad (\text{A.20})$$

The definition of the inverse of a matrix tells us that Eq. (A.6) is actually

$$T_{pq} = \Gamma_0^2 \left|(H_{eff}^{-1})_{qp}\right|^2 = \Gamma_0^2 \left|(G^R)_{qp}\right|^2. \quad (\text{A.21})$$

On the other hand, from Green's function method Eq. (25),

$$T_{pq} = (\Gamma_p)_{pp}(\Gamma_q)_{qq} \left|(G^R)_{qp}\right|^2, \quad (\text{A.22})$$

where  $(\Gamma_p)_{pp} = (\Gamma_q)_{qq} = \Gamma_0$ . Then Eq. (A.22) and (A.21) are same, the Bethe Ansatz method is equivalent to the Green's function method for determining the transmission coefficients. Moreover, the Bethe Ansatz method can also give the exact wave function.

- 
- [1] D. V. Averin and K. K. Likharev, in *Mesoscopic Phenomena in Solids*, edited by B. L. Altshuler, P. A. Lee, and R. A. Webb (Elsevier, Amsterdam, 1991).
- [2] M. A. Kastner, *Rev. Mod. Phys.* **64**, 853 (1992); *Phys. Today* **46**, 24 (1993).
- [3] U. Meirav and E. B. Foxman, *Semicond. Sci. Technol.* **10**, 255 (1995).
- [4] R. C. Ashoori, *Nature* **379**, 413 (1996).
- [5] C. W. J. Beenakker, H. V. Houten, and A. A. M. Staring, in *Single Charge Tunneling*, edited by H. Grabert and M. H. Devoret (NATO ASI Series B, Plenum, New York, 1991).
- [6] D. E. Chang, A. S. Sørensen, E. A. Demler, and M. D. Lukin, *Nat. Phys.* **3**, 807 (2007).
- [7] L. Zhou, Z. R. Gong, Y. X. Liu, C. P. Sun, and F. Nori, *Phys. Rev. Lett.* **101**, 100501 (2008).
- [8] A. Shnirman and G. Schøn, *Phys. Rev. B* **57**, 15400 (1998); Y. Makhlin, G. Schøn, and A. Shnirman, *Rev. Mod. Phys.* **73**, 357 (2001).
- [9] A. Hopkins, K. Jacobs, S. Habib, and K. Schwab, *Phys. Rev. B* **68**, 235328 (2003).
- [10] R. Ruskov, K. Schwab, and A. N. Korotkov, *Phys. Rev. B* **71**, 235407 (2005).
- [11] R. Lake and S. Datta, *Phys. Rev. B* **45**, 6670 (1992).
- [12] T. Koga, J. Nitta, H. Takayanagi, and S. Datta, *Phys. Rev. Lett.* **88**, 126601 (2002).
- [13] R. Citro and F. Romeo, *Phys. Rev. B* **77**, 193309 (2008).
- [14] R. A. Pepino, J. Cooper, D. Z. Anderson, and M. J. Holland, *Phys. Rev. Lett.* **103**, 140405 (2009).
- [15] R. Bhat, M. J. Holland, and L. D. Carr, *Phys. Rev. Lett.* **96**, 060405 (2006).
- [16] M. G. Sagnac, *Compt. Rend.* **157**, 708 (1913).
- [17] E. J. Post, *Rev. Mod. Phys.* **39**, 475 (1967).
- [18] M. Büttiker, *Phys. Rev. Lett.* **57**, 1761 (1986).
- [19] M. Y. Azbel, *J. Phys. C* **14**, L225 (1981).
- [20] M. Büttiker and Y. Imry, *J. Phys. C* **18**, L467 (1985).
- [21] R. Peierls, *Physik Z.* **80**, 763 (1933).

- [22] L. Jin and Z. Song, arXiv: 0906.5049.
- [23] J. B. Xia, Phys. Rev. B **45**, 3593 (1992).
- [24] S. Datta, *Electronic Transport in Mesoscopic Systems* (Cambridge University Press, Cambridge, 1995).
- [25] L. Amico, A. Osterloh, and F. Cataliotti, Phys. Rev. Lett. **95**, 063201 (2005).
- [26] S. F. Arnold, J. Leach, M. J. Padgett, V. E. Lembessis, D. Ellinas, A. J. Wright, J. M. Girkin, P. Öhberg and A. S. Arnold, Opt. Express **15**, 8619 (2007).
- [27] [http://en.wikipedia.org/wiki/Cramer's\\_rule](http://en.wikipedia.org/wiki/Cramer's_rule).